

## The Zodiacal Light from 1.0 to 0.3 A.U. as Observed by the Helios Space Probes

C. Leinert, I. Richter, E. Pitz, and B. Planck

Max-Planck-Institut für Astronomie, D-6900 Heidelberg-Königstuhl 1, Federal Republic of Germany

Received April 27, accepted June 22, 1981

**Summary.** In this paper we summarize the average properties of the zodiacal light as obtained from several years of observations from the Helios space probes.

The zodiacal light experiments on Helios 1 and Helios 2 give consistent results on intensity, colour and polarization of the zodiacal light between 1.0 and 0.3 A.U. The intensity increase towards the sun as a function of heliocentric distance is  $I(R) \sim r^{-2.3 \pm 0.05}$  where the upper and lower limits give the deviations observed at small and large elongations, respectively, from the sun. The colour is independent of heliocentric distance, slightly reddened with respect to the sun, particularly for small elongations. The polarization is somewhat higher than found from ground-based observations. It decreases towards 0.3 A.U. to about 2/3 of its value near the earth. No convincing explanation for this effect is found.

The results are interpreted in terms of a spatial distribution of interplanetary dust  $n(r, z) \sim r^{-1.3} \cdot f(|z/r|)$ , which could be an equilibrium distribution under the action of the Poynting-Robertson effect. The observed colours appear to exclude that a large fraction of the zodiacal light is due to submicron-sized particles. This as well as the absence of conspicuous changes for the regions closest to the sun suggests that collisions are not as dominating for the evolution of interplanetary dust as usually is assumed.

**Key words:** zodiacal light photopolarimetry – interplanetary dust – Helios space probes

### 1. Introduction

Before space experiments became available, observations of the zodiacal light and the F-corona were the main source of information on interplanetary dust and traditionally have been used to determine its spatial distribution and size spectrum. For example, Allen (1946) concludes that a dependence of number density with heliocentric distance  $n(r) \sim 1/r$  and a particle size with radius  $a \approx 10^{-3}$  cm would explain the observed brightness increase in the F corona. Van de Hulst (1947) and Elsässer (1955) determined size distributions for submillimeter particles of  $n(a) \sim a^{-2.6}$  and  $n(a) \sim a^{-2.0}$ , respectively, with a somewhat steeper increase of space density from 1.0 to 0.5 A.U. (Elsässer, 1958) and a large dustfree zone around the sun. Ingham (1961), with a continuously increasing spatial distribution  $n(r) \sim r^{-1.5}$ , found the exponent of the size spectrum to be  $-4.0$ , while Giese (1973), from Mie calculations for the light scattering of particles, limited the density increase towards the sun to less than  $n(r) \sim r^{-0.5}$ .

Send offprint requests to: C. Leinert

The discrepancies apparent in this short and necessarily incomplete overview demonstrate that earthbound observations alone are not able to determine the parameters of interplanetary dust. On the other hand, zodiacal light observations from a space probe, which penetrates the interplanetary medium, in principle allow a direct determination of the spatial distribution. Thus one of the main observational quantities relating to the dynamics of interplanetary dust can be obtained with considerable accuracy. In this paper we discuss the zodiacal light observations made on board the Helios 1 and 2 space probes between 1.0 and 0.3 A.U. with respect to the radial distribution  $n(r)$  of interplanetary dust. While the main result,  $n(r) \sim r^{-1.3}$ , already was extracted from a preliminary analysis of the raw data (Link et al., 1976), we present here the final data for an improved determination of the spatial distribution. This allows the reader to judge the reliability of our findings. In addition we summarize the quantitative results of the measurements performed near 1.0 A.U. and near 0.3 A.U., for comparison with other zodiacal light experiments, earthbound or on space probes, and for use in future model calculations.

The determination of particle properties including size distribution best can be accomplished by space experiments (Grün et al., 1980; Brownlee, 1978) and counts of microcraters on lunar rocks (Fechtig et al., 1974; Le Sergeant et al., 1980). However, zodiacal light observations provide an independent check on these results, and, when performed at different heliocentric distances, can be used to identify changes in the particle mixture. This discussion is closely connected to the determination of the spatial distribution and therefore also included.

This paper represents the concluding report on the average zodiacal light as observed in the 1975–1979 period with the Helios 1 and 2 space probes. The effects of the plane of symmetry of interplanetary dust have been discussed by Leinert et al. (1980). The questions of short-term and long-term variations of zodiacal light will be treated separately.

### 2. Instrument

The experiment and its calibration have been described in some detail previously (Leinert et al., 1975, 1981; Pitz et al., 1976). It consists of 3 independent telescope-photometer systems, mounted at fixed angles of 16, 31, and 90° to the spacecraft equatorial plane (nominally the ecliptic plane), with respectively 1°, 2°, 3° fields-of-view. Each photometer records brightness and polarization sequentially in *U*, *B*, *V* spectral bands. The one-second spacecraft spin is divided into 32 sectors of 5°6, 11°2 or 22°5 in length. Data from 513 spins are accumulated and averaged before telemetry. The experi-

ment operates continuously, with one complete cycle through all filter-photometer combinations requiring  $\approx 5$ h. On Helios 1 the telescopes point South of the ecliptic; on Helios 2 they point North of the ecliptic.

Helios 1, launched on December 10, 1974, still is in operation, now in its seventh year. Helios 2 was active from January 15, 1976 until March 1980. The perihelion distances are 0.31 and 0.29 A.U., respectively, corresponding to orbital periods of 190 and 185 d. The aphelia are at 0.984 A.U.

The calibration is based with equal weight on preflight laboratory measurements and on in-flight observations of bright star crossings. The agreement between the two methods is better than 10%. Finally we adopted errors in the intensity measurements of  $\pm 6\%$  in  $U$ ,  $\pm 4-5\%$  in  $B$  and  $V$ , while the colours and the comparison between different sensors should be accurate to  $\pm 3-4\%$ . As expected from laboratory measurements (Leinert and Klüppelberg, 1974), instrumental stray light was negligible (Leinert et al., 1981). Because the sun is the light source giving rise to the zodiacal light we calibrated the experiment in S10 units (equivalent number of  $V=10.0$  solar type stars per square degree), following the recommendations by Sparrow and Weinberg (1976), i.e.  $V_{\odot} = -26.73$ ,  $(B-V)_{\odot} = 0.63$ . The solar  $(U-B) = 0.15$  was taken from Gallouet (1964).  $S_{10}(B)$  and  $S_{10}(U)$  units are larger than the corresponding S10 units by factors of 1.79 and 2.05, respectively.

Complete zodiacal light measurements were possible throughout the mission of Helios 2 and on Helios 1 until November 1976, when the filter wheel motors started getting stuck. For this paper we selected from the first two years of each spacecraft intervals with good data coverage and nearly constant spin axis orientation, the  $-z$ -axis (photometer  $90^{\circ}$ ) being tilted  $\approx 0.5^{\circ}$  towards the sun for Helios 1 and  $\approx 0.5^{\circ}$  away for Helios 2. Such a choice is uncritical because the measurements were repeatable from orbit to orbit within a few percent throughout the mission. The scatter in the raw data typically is less than 1%.

### 3. Data Reduction

#### 3.1. Brightness

The calibration includes the effects of temperature, non-linearity and varying spacecraft spin. After subtracting the dark current of  $\approx 400$  counts per s at the photomultiplier, which is a few percent of a typical signal near 1 A.U., we obtain what we call reduced data. From these the stellar background and the contribution of interplanetary plasma have to be removed to obtain the zodiacal light data.

Bright stars in the field of view, as given in the Bright Star Catalogue (Hoffleit, 1964) and the Naval Observatory Photoelectric Catalogue (Blanco et al., 1968), were individually subtracted to limiting magnitude  $V=6.5$ ,  $B=7.13$ ,  $U=7.28$ , corresponding to a solar type spectrum. The magnitude limit is at a level where the catalogues still are essentially complete and fits the magnitude limits used in star background work.

For galactic latitudes  $|b| < 20^{\circ}$   $UBV$  brightness of the milky way were derived from the Helios measurements themselves (Leinert and Richter, 1981). The star background for medium galactic latitudes was based, in  $B$ , on the milky way photometry by Classen (1976), which has a limiting magnitude of  $B \approx 7$  in the milky way and  $B=8.0-8.5$  at higher latitudes. This approach is supported by the fact that in the milky way Classen's results agree very well with the Helios data. Since the agreement with the UV-photometry of Pfeleiderer and Mayer (1971) is not as good, and since

a comparable photometry in  $V$  is missing, we calculated the star background in these wavelength bands for  $|b| > 20^{\circ}$  from the  $B$  values, using the colours  $U-B=0.23$ ,  $B-V=0.70$  as given by Mattila's (1980) synthetic model of the integrated starlight. The agreement at low latitudes between the Helios observations and the colours predicted by the model were taken as justification for this procedure.

For  $|b| > 50^{\circ}$  we adopted, in  $B$ , the average of star counts for  $m \geq 6.1$  mag (Roach and Megill, 1961) and  $m \geq 8.0$  mag (Sharov and Lipaeva, 1973). Again, values for  $U$  and  $V$  were derived with the help of Mattila's model.

The scattering by the electrons of the interplanetary plasma was calculated from the spatial distribution

$$n_{el} = 7.4 \times (1 \text{ A.U./}r)^{2.2} \text{ cm}^{-3} \quad (1)$$

which Edenhofer et al. (1976) derived from an analysis of the Helios telemetry signals. This represents a large scale average in the ecliptic during the minimum of solar cycle 1975/76, the time interval to which most of our data refer. A gradual decrease of plasma density outside the solar equatorial plane was added, calculated on the assumption of constant flux from the velocity increase with heliographic latitude  $\phi$

$$V(\phi) = 425 + 2.1 \phi \text{ (}^{\circ}\text{) km s}^{-1} \quad (2)$$

which is an average of what Coles and Rickett (1976) found from interplanetary scintillations during the period 1971-1975. The well known scattering function for electrons is

$$S_1(\vartheta) = \frac{1}{2} \left( \frac{e^2}{mc^2} \right)^2, \\ S_2(\vartheta) = \frac{1}{2} \left( \frac{e^2}{mc^2} \right)^2 \cdot \cos^2 \vartheta \quad \text{cm}^2 \text{ sterad}^{-1} \text{ (cgs-units)}, \quad (3)$$

where  $\vartheta$  is the scattering angle and the subscripts refer to scattering of the incoming unpolarized light perpendicular and parallel to the scattering plane. The resulting correction usually is very small, except for viewing directions at small angular distances to the sun, where it reaches 10% of the total signal in perihelion.

The position of the fields of view on the sky, as given by the known spin axis orientation and the mounting of the experiment into the spacecraft, was checked by bright stars drifting across the boundaries. After the resulting small ( $0.01-0.1^{\circ}$ ) corrections in photometer elevation the positions in general appear to be accurate to better than  $0.1^{\circ}$ .

Tapes with reduced data as well as with zodiacal light data are available from the National Space Science Data Center, Goddard. These also contain the results on zodiacal light polarization.

#### 3.2. Polarization

This was the only tough task in the Helios data evaluation, and some manipulation was necessary before the data appeared credible to us. There is no problem with photometer  $90^{\circ}$ , which, by the spacecraft spin, is rotated once per second about its optical axis. Insertion of a polarizing foil leads to a modulation of transmitted intensity with twice the spin frequency, from which the polarization is extracted by the standard method of measuring in eight  $45^{\circ}$  intervals.

In the other photometers polarization is being determined by consecutive measurements through three polarizing foils, oriented at  $0^{\circ}$ ,  $45^{\circ}$ , and  $90^{\circ}$  with respect to the spacecraft equatorial plane.

For each sector we thus obtain measured signals in S10 units,  $S_0$ ,  $S_{45}$ , and  $S_{90}$ , from each of which the contributions of stellar background and interplanetary plasma are subtracted. For the latter correction which consists of light polarized by typically 60% perpendicular to the scattering plane we have to take care of the actual orientation  $\varphi$  and polarizing ability  $q$  of each individual polarizing foil. Values for  $q$  were 0.81–0.92 in  $U$ , 0.75–0.97 in  $B$ , 0.96–0.99 in  $V$ . The resulting corrected signals  $S_0^c$ ,  $S_{45}^c$ ,  $S_{90}^c$  are related to the Stokes parameters  $I_{zi}$ ,  $Q_{zi}$ ,  $U_{zi}$  of the zodiacal light by the equations

$$\begin{aligned} S_0^c &= I_{zi} + Q_{zi} q_0 \cos 2\varphi_0 + U_{zi} q_0 \sin 2\varphi_0 \\ S_{45}^c &= I_{zi} + Q_{zi} q_{45} \cos 2\varphi_{45} + U_{zi} q_{45} \sin 2\varphi_{45} \\ S_{90}^c &= I_{zi} + Q_{zi} q_{90} \cos 2\varphi_{90} + U_{zi} q_{90} \sin 2\varphi_{90}, \end{aligned} \quad (4)$$

where  $\varphi_0$ ,  $\varphi_{45}$ ,  $\varphi_{90}$  give the actual orientation of the polarizing foils with respect to the spacecraft equatorial plane as measured on ground. The equations were solved for the Stokes parameters to give the degree of polarization

$$p = \frac{(Q_{zi}^2 + U_{zi}^2)^{1/2}}{I_{zi}} \quad (5)$$

and angle of polarization

$$\theta = \frac{1}{2} \arctan \left( \frac{U_{zi}}{Q_{zi}} \right) \quad (6)$$

of the zodiacal light. By simple spherical geometry  $\theta$  is transformed into an angle relative to the scattering plane.

Two unexpected difficulties appeared:

First we noticed that even in perihelion, where background corrections are small, the calculated polarization showed several unwanted features (see Fig. 1):

- The direction of polarization deviated by about  $5^\circ$  from the expected direction normal to the scattering plane. This effect was not symmetric with respect to the sun.
- The degree of polarization at equal angular distances east or west of the sun was different by several percent.
- The polarization near the antisolar direction still was up to several percent.
- Bright stars showed polarizations of 2–3%.

Instrumental scattered light and star background were excluded as source of the trouble. Tests on the spare unit did not show such a malfunction. Since the effects were repeatable from orbit to orbit we decided it was an instrumental effect, some parameters being different in flight with respect to the laboratory calibration.

From Eq. (4) we found that the only parameters on which the result depended strongly were the relative calibration of the signals  $S_0$ ,  $S_{45}$ ,  $S_{90}$ . Accordingly, for each photometer and each colour we varied the relative calibration of  $S_{45}/S_0$  and  $S_{90}/S_0$  independently in steps of 0.5% and calculated the polarization of zodiacal light in perihelion, including the contribution of interplanetary plasma. We then determined, for each point of the resulting grid, the average deviation of the direction of polarization from the nominal value perpendicular to the scattering plane, for the eight sectors east and west of the sun which are at less than  $50^\circ$  elongation. We judged that this quantity,

$$D = \left( \frac{1}{16} \sum_{i=1}^{16} \Delta\theta_i^2 \right)^{1/2} \quad (7)$$

would be least affected by uncertainties in star background or three dimensional distribution of interplanetary dust. We adopted that change in relative calibration which minimized the deviation  $D$ . For the case shown in Fig. 1 this was a 2% change in the relative calibration

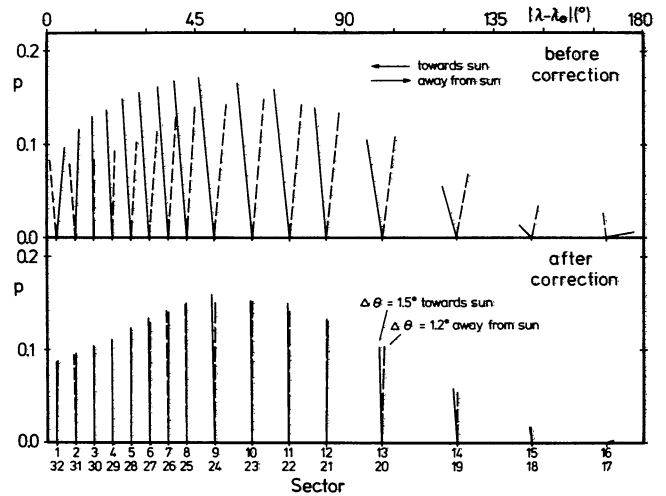


**Fig. 1.** Effect of the correction in relative transmission of the polarization foils in Helios 2, photometer  $15^\circ V$ . Data are from day 108/1976, measured in perihelion ( $R=0.29$  A.U.). Polarization for each sector is given by a bar (— east, --- west of the sun), the length of which gives the degree of polarization. The direction of polarization with respect to the scattering plane is given by the direction of the bar, perpendicular orientation corresponding to the nominal direction perpendicular to the scattering plane. In this case the relative calibration  $S_{45}/S_0$  was changed by a factor of 0.98

tion  $S_{45}/S_0$ , retaining the relative calibration  $S_{90}/S_0$ . Now the directions of polarization showed an offset of  $+1^\circ$  (counter clockwise on the sky). Since this effect appeared in all photometers and colours considered here, we took it for real and corrected for it. Instrumental reasons for this, although small, effect could be an error in our test equipment or, more probably, a change from the idle position during tests on ground to the rapid spinning in flight. Finally the following improvements were achieved (numbers in  $a, b, c$  referring to Fig. 1):

- The direction of polarization for  $\epsilon < 50^\circ$  could nearly be forced into nominal direction, with  $D=0.4^\circ$  instead of  $D=3.7^\circ$ . But also for other sectors and for observations at other heliocentric distances no systematic deviation remained.
- The difference in degree of polarization east and west of the sun effectively disappeared, changing from 0.037 to 0.002 in perihelion, being reduced below 0.01 also in aphelion.
- The degree of polarization near the antisolar direction was reduced from 2.6% to 0.4% in perihelion and similarly in aphelion.
- The polarization in the signal of bright stars decreased from 2–3% to  $\approx 0.5\%$ .
- As should be expected, the polarization data now were smoothest in  $V$  and showed the largest scatter in  $U$ .

This general behaviour increased our confidence that we were correcting for a real effect and not forcing the data into an arbitrary mould. The corrections necessary in the relative calibrations of the polarizing foils in the average were 1.3% with a maximum of 3.0% in the ratio  $S_{90}/S_0$  in  $U$  of photometer  $16^\circ$  of Helios  $B$ .

The above procedure is not as arbitrary as might appear at a first glance. The transmission of one of the polarizing foils in photometer  $16^\circ$  is being checked by a monitoring lamp. It showed a decrease by 2% with respect to ground-based operation. In addition, the average transmission of the three polarizing foils in one photometer can be determined by comparing the zodiacal light intensities observed through a naked colour filter with that resulting

**Table 1.** Error propagation in polarization measurements with fixed orientations of the polarizing foils

Experimental setup	$\Delta p$ for $p \gg \Delta M/M$	Measured $p$ for $\Delta p \approx 0$
Four foils at $0^\circ, 45^\circ, 90^\circ, 135^\circ$	$\frac{1}{\sqrt{2}} \Delta M/M$	$\Delta M/M$
Three foils at $0^\circ, 45^\circ, 90^\circ$	$\frac{1}{\sqrt{2}} \sqrt{(1 + 2 \sin^2 2\theta)} \Delta M/M$	$\sqrt{2} \Delta M/M$
Three foils at $0^\circ, 60^\circ, 120^\circ$	$\sqrt{\frac{2}{3}} \Delta M/M$	$\frac{2}{\sqrt{3}} \Delta M/M$

$\Delta M$  is the error of an intensity measurement  $M$

from Eq. (4). The measurements with polarization foil were lower by 2% in  $V$ , 6% in  $B$ , 9% in  $U$  for photometer  $16^\circ$  of Helios 2 and by a somewhat smaller amount for Helios 1. We blame slight differences in the degradation of the polarizing foils and slight errors in the laboratory calibration of their relative transmission for the corrections discussed above. To summarize, we calculated polarizations from Eq. (4) only after two corrections to the signals  $S_0$ ,  $S_{45}$ ,  $S_{90}$ : a correction to the relative calibration as discussed above and a correction to the absolute calibration of all three polarizing foils taking care of the observed decrease in transmission.

The second unexpected difficulty was the large scatter in the degree of polarization observed in photometer  $16^\circ$  in aphelion at large angular distances from the sun. In these cases the zodiacal light signal in  $U$  with polarizing foil may be as low as 450 counts per second at the photomultiplier, only slightly higher than the dark count rate, and about twice this value in  $B$  and  $V$ . The scatter in the dark current, which in flight increased to about 10 times the value expected from statistics, then gave rise to spurious "observed" polarizations of up to 10–20%. Averaging the Stokes Parameters of 5–10 subsequent measurements reduced this noise to a level where meaningful polarizations could be derived also for the least luminous parts of our strips on the sky.

The orientation of the polarization foils at  $0^\circ$ ,  $45^\circ$ , and  $90^\circ$  proved to be convenient for testing of the instrument and quick look of the flight data. Table 1 shows that virtually no disadvantage in accuracy occurs when compared to a regular spacing in  $60^\circ$  intervals.

## 4. Results

### 4.1. Intensity

Even if the zodiacal light were perfectly constant in time the Helios photometers would notice a temporal change for the following reasons:

a) The intensity strongly depends on the heliocentric distance of Helios, the increase towards the sun being  $I(R) \sim R^{-2.3}$ .

b) Because of the tilt of the plane of symmetry of interplanetary dust with respect to the ecliptic ( $i = 3.0^\circ$ ,  $\Omega = 87^\circ$ , Leinert et al., 1980) there is an asymmetry between observations east and west of the sun which varies along the orbit of Helios approximately proportional to  $\cos(\lambda_{\text{Helios}} - \Omega)$  (see Leinert et al., 1980, Figs. 4 and 5).

The size of this effect, up to  $\pm 7\%$ , was determined individually for each sector from Helios 2 observations, when the spacecraft was in the node. It was assumed that the effect had the same size for Helios 1. This effect only applies to sensors  $15^\circ$  and  $30^\circ$ .

c) The motion of Helios with the respect to the plane of symmetry still leads to a modulation of the average of observations east and west of the sun, now approximately proportional to  $\sin(\lambda_{\text{Helios}} - \Omega)$  (Dumont and Levasseur-Regourd, 1978). From Helios this cannot be observed directly, but inferred from the difference between observations on the ingoing and outgoing branch of the orbit, which is approximately proportional to  $\sin(\lambda_{\text{Helios}} - \lambda_{\text{aphelion}})$ . Among these two modulations the second, observable one is smaller by a factor  $\cos(\Omega - \lambda_{\text{aphelion}})$ , as follows from the geometric relation of the angles involved. The observed variation for Helios 2 was  $\pm 6\%$  in sensor  $15^\circ$ ,  $\pm 8.5\%$  in sensor  $30^\circ$ . For sensor  $90^\circ$  the modulation of  $\pm 3.8\% \cdot i^\circ$  was taken from Dumont and Levasseur-Regourd (1978). It was assumed that the effect had the same size for Helios 1, except for the correction for the different longitude of aphelion.

d) Any change in spin axis orientation moves the field of view on the sky, changing the observed zodiacal light intensity. A rotation of the spin axis around the sun-Helios-line leads to an asymmetry in observations east and west of the sun. Since the effect of the  $3^\circ$  tilt of the plane of symmetry is known, any such rotation of the spin axis also can be corrected for. For a tilt of the spin axis towards or away from the sun we read the correction factor between the intensity in the actual field of view and that expected for nominal spin axis orientation from the table given by Dumont and Sanchez (1976). For  $\varepsilon < 30^\circ$  this factor was determined by model calculations. Applying corrections b)–d) to our data, we obtain, what we call normalized intensities as they would be observed by an observer in the plane of symmetry at a latitude of  $|\beta| = 16.2^\circ, 31.0^\circ$  or  $90^\circ$  with respect to that plane. We judged that these quantities best would be comparable with other results. Unless otherwise indicated we are using normalized intensities in this paper. Scaling to a heliocentric distance different from that of the observations is done with a factor  $R^{-2.3}$ .

Alternatively, the factor transforming observed into normalized intensities also can be derived by model calculations, using the parameters of the symmetry plane  $\Omega = 87^\circ$ ,  $i = 3^\circ$ , a spatial distribution of dust

$$n(r, z) = r^{-1.3} \exp(-2.1 |z/r|) \quad (8)$$

and the corresponding "empirical" scattering function (see Leinert et al., 1976). With the parameters of the symmetry plane given above the two approaches agree within 1–2%.

Figure 2 shows the Helios results "at" 1 A.U. compared with earthbound observations. Each point given for Helios is an average over a period of two to three weeks around aphelion (0.984 A.U.) as read from a plot of normalized intensities, averaged again over several aphelion transits. Also observations east and west of the sun, which showed no systematic difference, were averaged. The resulting normalized intensities for  $R = 1.0$  A.U. given in the Figure refer to model calculations according to Eq. (8) because we felt this normalization would be more meaningful to the reader than the empirical relations a)–d) which are based on data not presented here in detail. It is reassuring to see the north-south symmetry of zodiacal light reflected in the agreement of Helios 1 with Helios 2. Frey et al's (1974) results are higher by about 15% which would be in accordance with the reddening of zodiacal light discussed below. By the same argument, the values of Levasseur-Regourd and Dumont (1980) should be a little lower than the Helios values,

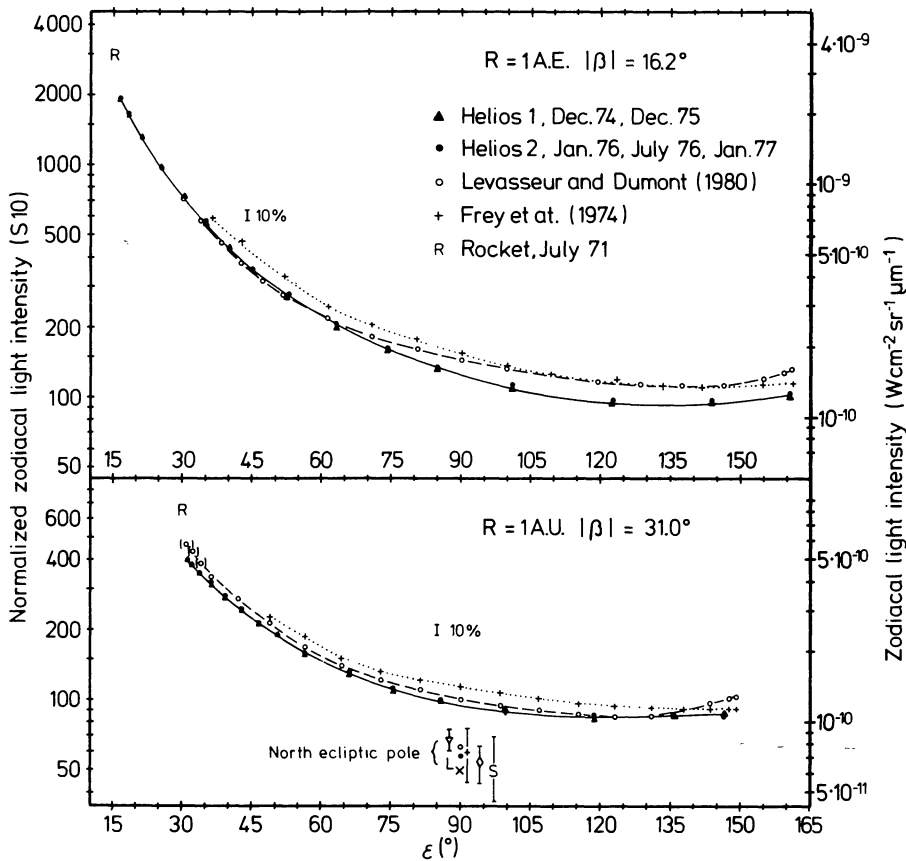


**Fig. 2.** Comparison of zodiacal light intensities observed by Helios in  $V$  near 1 A.U. with other observations. Effective wavelengths are: Helios 529 nm, Levasseur-Regourd and Dumont (1980) 502 nm, Frey et al. (1974) 710 nm, Rocket (Leinert et al., 1976) 592 nm. Helios results are normalized intensities for an observer at 1 A.U. For the north ecliptic pole the available results of satellite experiments were included:  $S$  [OSO-2, Sparrow and Ney (1968), in  $V$ ],  $L$  [OAO-2, Lillie (1972),  $\lambda_{\text{eff}} = 425$  nm],  $\diamond$  [OSO-5, Sparrow and Ney (1972),  $\lambda_{\text{eff}} = 418$  nm],  $\nabla$  [D2B, Levasseur and Blamont (1976),  $\lambda_{\text{eff}} = 653$  nm],  $\times$  [Skylab, June 73, Weinberg and Hahn (1980),  $\lambda_{\text{eff}} = 643$  nm]. Parentheses around values at small  $\varepsilon$  are from authors

which generally is not the case. But still the agreement is quite satisfactory.

The Helios results at the north ecliptic pole strongly depend on the adopted star background and calibration. Since Classen's (1976) photometry does not cover this region the star background in  $B$  was taken from the star counts, which give a value of 52 S10 at the north ecliptic pole. Since the observations of photometer 90° always are made through a polarizing foil, a correction for decreased

transmission of this foil was applied as determined from photometer 15° of the same spacecraft (see Chapt. 3.2). A one percent change in calibration results in a 1.0–1.2 S10 (for  $U$  and  $V$ , respectively) change in intensity. This is demonstrated in Table 2, which also includes other photopolarimetric observations for comparison. Concerning the results of OSO-5, Burnett (1976) found that the calibration should be revised upwards by about 10%.

The intensities observed in perihelion were evaluated in the same way as those in aphelion. They are presented in Fig. 3, normalized [with Eq. (8)] to a heliocentric distance of Helios of  $R = 0.3$  A.U. Again Helios 1 and Helios 2 essentially give the same results. The difference of less than 1% at  $|\beta| = 16^\circ$  is smaller, while the difference of 6% at  $|\beta| = 31^\circ$  is a little larger than expected from calibration accuracies. However, uncertainties in temperature correction and imperfections in the model of Eq. (8) or the parameters of the symmetry plane also may contribute to the small difference. The value at the south ecliptic pole is not considered very reliable, because of the proximity of the Large Magellanic Cloud to the field of view. Temporal changes, if any measurable exist, are small and will be discussed elsewhere.

As may be seen from a comparison of Fig. 2 and 3, the brightness profiles of the zodiacal light change only very little from aphelion to perihelion. This is further demonstrated in Fig. 4 which gives, for Helios 2, brightness profiles for different heliocentric distances.

For the interpretation of brightness changes with heliocentric distance in terms of distribution of interplanetary dust it is important to know whether the relative brightness increase the sun is the same for all viewing directions. This can best be judged from Fig. 5. There we present data from the sensors of Helios 1 and 2 for different elongations. All individual intensity measurements performed during one orbit are given without smoothing, normalized to

**Table 2.** Zodiacal light at the north ecliptic pole at 1 A.U.

	$U$	$B$	$V$
Normalized intensity as observed	44 S10	47 S10	55 S10
After transmission correction	52 S10	53 S10	57 S10
Corrected to standard $UBV$	52 S10	54 S10	57.5 S10
Polarized intensity	10.8 S10	13.1 S10	11.1 S10
After transmission correction	11.6 S10	13.9 S10	11.3 S10
$p$ observed	0.245	0.279	0.203
After transmission correction	0.225	0.262	0.199
Dumont and Sanchez (1976)			63 S10 (502 nm)
$I_p$			11.3 S10
$p$			$0.18 \pm 0.02$
OSO-5, OSO-2		$54 \pm 10$ S10	$50 \pm 20$ S10
Sparrow and Ney (1972, 1968)		$10.9 \pm 1$ S10	$10.5 \pm 1$ S10
$p$		$0.20 \pm 0.04$	$0.21 \pm 0.08$
Skylab (South ecliptic pole)			50 S10 (643 nm)
Weinberg and Hahn (1980)			$11.4 \pm 0.5$ S10
$p$			0.228

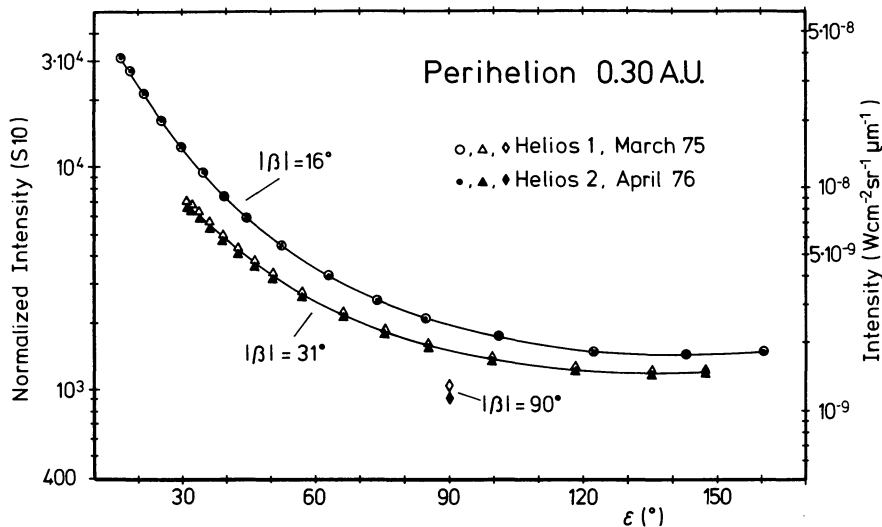


Fig. 3. Zodiacal light intensities at perihelion. Given are the Helios observations in  $V$  normalized to 0.3 A.U. The effective wavelength is 529 nm

1 A.U. according to corrections a)–d). This means, if the brightness increase towards the sun were strictly  $R^{-2.3}$  and if we applied the right corrections for the effects of spacecraft tilt and symmetry plane, the points should all lie on a horizontal straight line. In fact this is essentially what we observe. Nevertheless the slight deviations also should be noticed. In general the effects of the symmetry plane have adequately been corrected for, i.e. measurements on the ingoing and outgoing parts of the orbit coincide. However, there is a slight overcorrection in photometer 90°, while in a few cases also noticeable undercorrections occur, e.g. in photometer 15 of Helios A at  $\varepsilon = 17^\circ$ . The brightness increase towards the sun is slightly steeper than  $R^{-2.3}$  for elongations  $\varepsilon < 60^\circ$ , but typically still by less than 13%, which would correspond to a change by 0.1 in the exponent of the power law. As in Fig. 3, the values of sensor 30° in Helios 1 rise strongest towards perihelion, as would be the case if the temperature correction was off by a few percent. The brightness increase is slightly weaker than  $I(R) \sim R^{-2.3}$  at large elongations. There of course the values at 1 A.U. strongly depend on the adopted brightness of the star background.

In summary, however, we want to stress how closely the intensity changes  $I(R)$  are the same for all viewing directions. Based on laboratory calibration alone the brightness increase towards the sun would have been larger by 2–3%, based on star crossings alone lower by the same amount.

#### 4.2. Colour

The observed colour of zodiacal light does not show a change with heliocentric distance (Fig. 6). In general it is redder than the sun as shown most clearly in perihelion (Fig. 7). These data support the accuracy of 3–4% derived from calibration for the ratios  $I_V/I_B$  and  $I_B/I_U$ . Obviously the amount of reddening is increasing at small elongation from the sun. The results for aphelion are quite similar (Fig. 8). In particular they show the same reddening at small elongations and the decreasing deviation from solar colour towards large elongations. The low values of  $I_B/I_U$  at large elongations indicate a slight change with respect to the perihelion observations, but in view of the low zodiacal light values in aphelion and the resulting importance of star background we hesitate to declare it an observed change. Other observers usually find their observations compatible with a solar colour of zodiacal light (Frey et al., 1974; Dumont and Sanchez, 1975; Weinberg and Hahn, 1980). Their observations mostly refer to medium and large elongations, where we find the reddening decreasing. Within the errors of their measurements their results appear also to be compatible with our findings. The reddening at elongations  $\varepsilon < 60^\circ$  of the order of 10% per 100 nm, which we also found in earlier rocket experiments, and the decrease of reddening with increasing angular distance from the sun are among the clear and pronounced features in our zodiacal light observations. Based on laboratory calibration alone, the reddening would have been 2.4% less from  $B$  to  $V$  and 1.4% less from  $U$  to  $B$ , based on calibration by stars only the reddening would have to be increased by the same amount.

#### 4.3. Polarization

The only striking qualitative change in zodiacal light we found is the steady decrease of the degree of polarization towards perihelion to 2/3 of its aphelion value, and even less for the viewing directions closest to the sun (Fig. 9a). A wrong correction for electron scattered

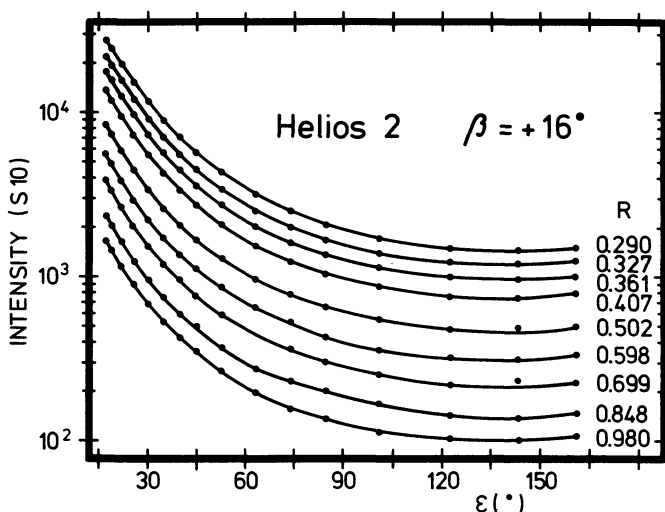


Fig. 4. Brightness profiles of the zodiacal light during the first half of the first orbit of Helios 2. Observations east and west of the sun were averaged, but no correction for the effect of the plane of symmetry or slight deviations of spin axis applied

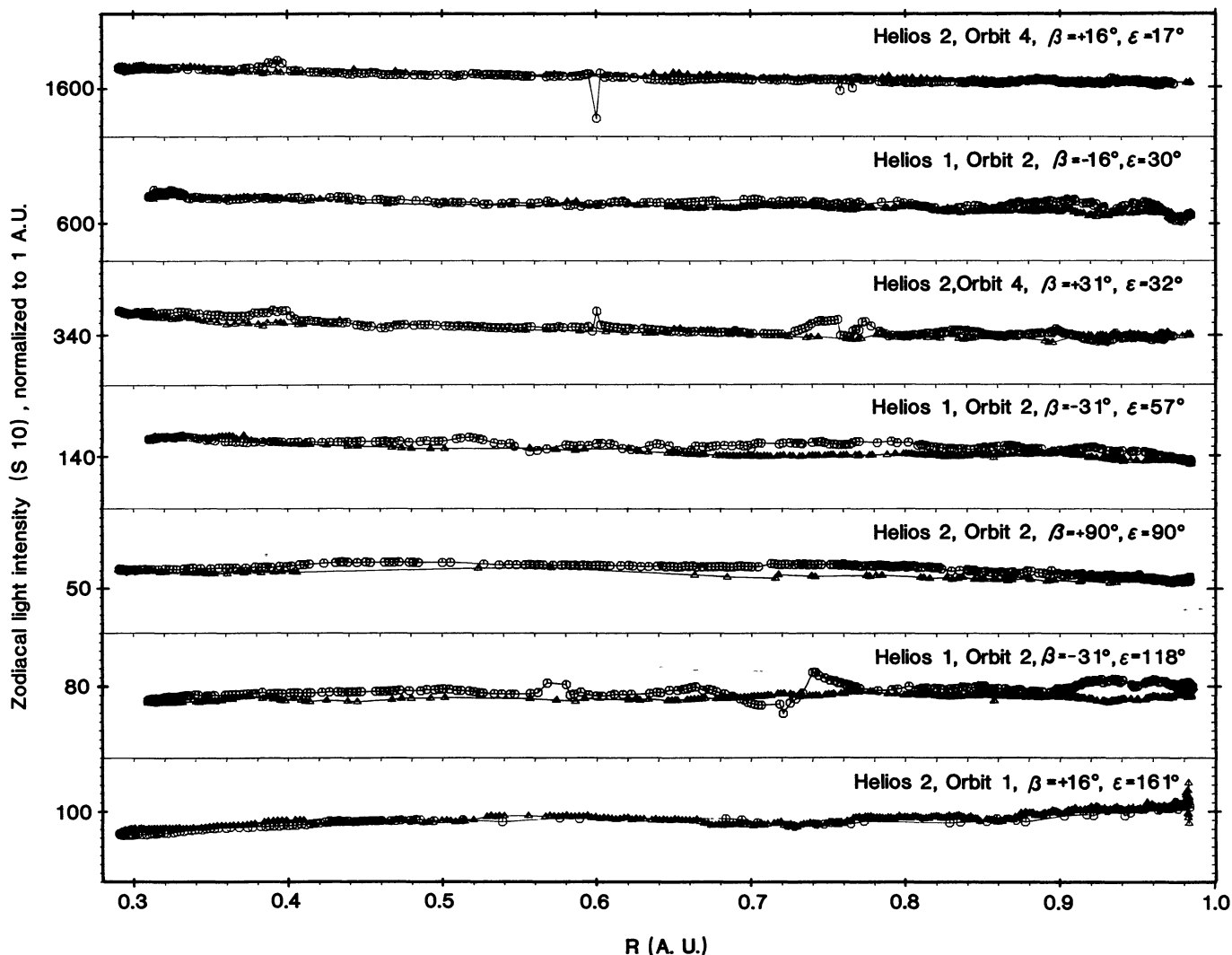
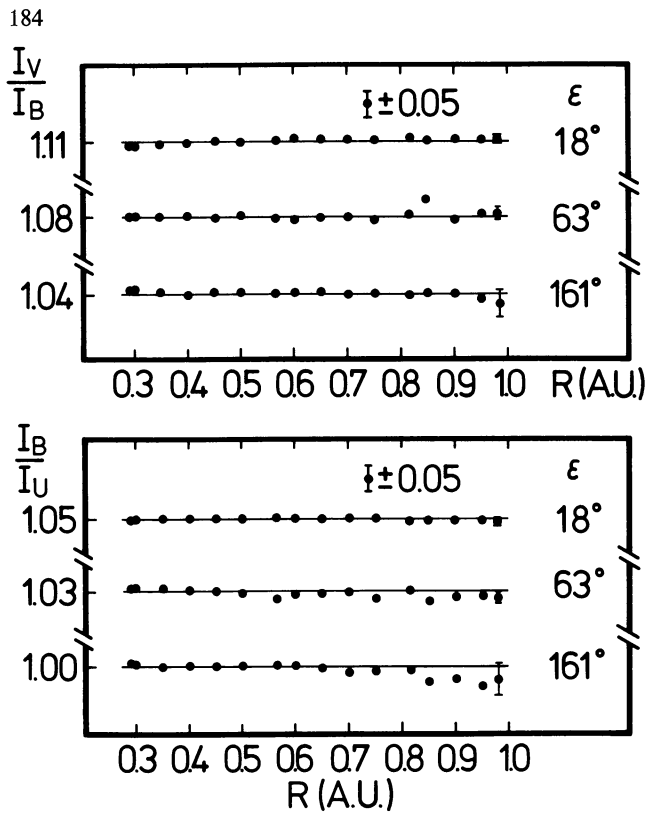


Fig. 5. Brightness increase of zodiacal light in  $B$  towards sun for different viewing directions relative to a power law  $I(R) \sim R^{-2.3}$ .  $\Delta$  refers to inbound,  $\circ$  to outbound part of orbit.  $\lambda_{\text{eff}}$  of observations is 425 nm, 1 S10 corresponding to  $1.02 \cdot 10^{-12} \text{ W cm}^{-2} \text{ sterad}^{-1} \mu\text{m}^{-1}$ . For each viewing direction the step size of ordinate division is 5% of the given intensity value

light could mimic such an effect, but this is excluded by the fact that even before this correction is applied the values do show the same qualitative behaviour. We also exclude a change in the polarizing ability of the polarizing foils as source of the decrease in polarization. The temperature in perihelion is near room temperature where the foils are effective by 81–99%. In addition the sensor viewing the north ecliptic pole detected highly ( $p \approx 100\%$ ) polarized plasma clouds over the whole range of heliocentric distances. And in this viewing direction the typical decrease in polarization towards perihelion was observed, too, from 0.225 to 0.180 in  $U$ , from 0.262 to 0.190 in  $B$ , and from 0.199 to 0.137 in  $V$ .

More quantitative detail is given in Fig. 10, which compares observations in aphelion and perihelion and also includes the results of other authors. The run of the polarization with elongation is similar to that found by Dumont and Sanchez (1976), but their values are markedly lower than the Helios observations near 1 A.U. This also is true – to a lesser extent – for their observations at the north ecliptic pole and the comparison with other space observations (see Table 2).

The wavelength dependence of the degree of polarization in the Helios data, i.e. low values in  $V$ , high values in  $U$ , only in part is a “result” of the reddening discussed in Sect. 4.2. The polarized intensity also is increasing, for example at  $|\beta| = 16^\circ$ ,  $\epsilon = 45^\circ$  near aphelion from 69 S10 in  $V$  to 76 S10 in  $U$ . As with the degree of polarization, the values in  $B$  were found intermediate from Helios 2 and slightly larger than in  $U$  from Helios 1. Since we are not able to blame one of the measurements for this apparent systematic error we suggest to take the average of Helios 1 and 2 measurements as most reliable representation of the true zodiacal light. At the north ecliptic pole we also found the highest polarization in  $B$ . The shape of the polarization curve and the wavelength dependence of polarization appear most clearly in the perihelion data, which, for  $|\beta| = 16^\circ$  are summarized in Fig. 11. At a first glance the results are at variance with Weinberg and Hahn (1980) and Sparrow et al. (1976) which both stress that the polarized intensity is close to the solar colour. However, their conclusion refers to the wavelength region 475–709 nm. At 400 nm they also find a higher polarization, which they attribute to difficulties with calibration. We



**Fig. 6.** Colour of zodiacal light relative to solar colour observed with Helios 2 at  $\beta=16^\circ$  during the ingoing part of the first orbit. Numbers larger than 1.0 signify a reddening of the zodiacal light. The error bars with the aphelion points show the influence of an uncertainty of  $\pm 0.1$  in  $B-V$  and  $U-B$  of the star background. Values refer to individual measurements selected for regular spacing in  $R$

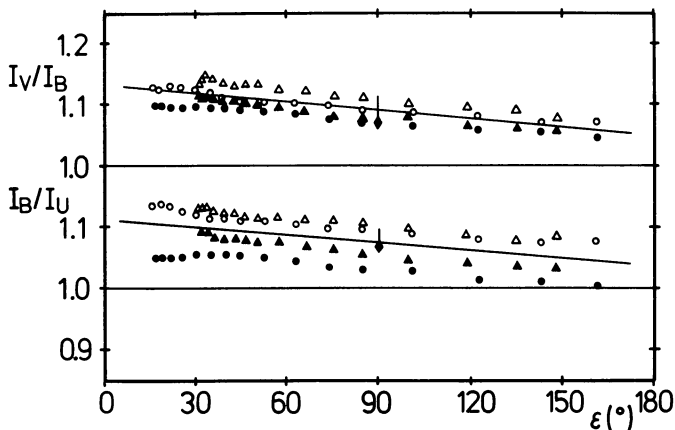


**Fig. 7.** Colour of the zodiacal light relative to solar colour observed in first perihelion. Symbols  $\bullet$ ,  $\blacktriangle$ ,  $\blacklozenge$  refer to  $\beta = +16^\circ$ ,  $+31^\circ$ ,  $+90^\circ$  (Helios 2), open symbols to the corresponding negative ecliptic latitudes (Helios 1). The bar on the point at  $\varepsilon=90^\circ$  indicates by how much the colour changed because of the correction for decreased transmission of polarizing foils. The discrepancy in  $I_B/I_U$  between observations at  $\beta = +16^\circ$  and  $\beta = -16^\circ$  probably is due to differences in the coatings of the folding mirrors occurring in these sensors. Straight lines are least square fits

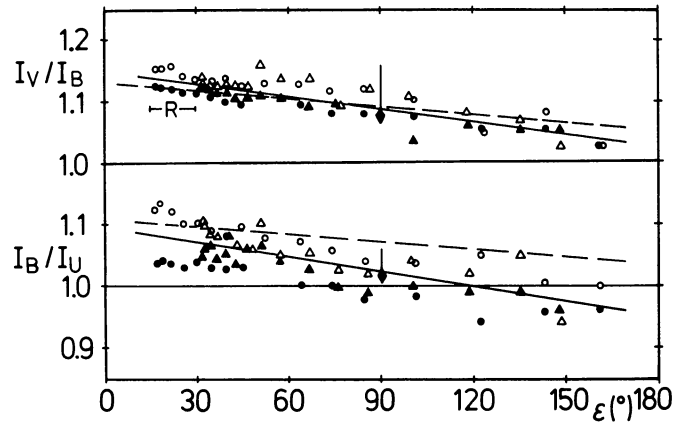


**Fig. 8.** Colour of the zodiacal light relative to solar colour observed at 1 A.U. six days after launch. Symbols are the same as in Fig. 7. For comparison, the perihelion straight line fits also are given (---).  $R$  refers to the average of earlier Rocket experiments (Leinert et al., 1976; Pitz et al., 1979). The time period was selected to avoid the initial attitude maneuvers

suggest that they were observing the same increase of polarization towards short wavelengths we found in our data.

The direction of polarization agrees with the expected value perpendicular to the scattering plane within a few degrees, as in the examples shown in Fig. 9a and b, and often better. In the range of elongations available it is only at  $\varepsilon=161^\circ$ , where  $p$  is less than 0.01, that a turnover of the direction of polarization into the scattering plane is indicated. But the data are too noisy to put much weight on it.

So far we found no evidence for systematic temporal changes of polarization except small effects due to the variation of interplanetary plasma. The scatter in individual polarization measurements is increasing from  $V$  to  $U$ , distinctly less than 1% in the bright parts of the zodiacal light and greatly increasing in the dim parts because of the influence of the dark current. For averages like in Figs. 10 and 11 essentially the systematical errors remain. In comparing Helios 1 and 2 the difference typically is 1%, with a maximum of  $\Delta p=0.027$  in  $B$  at  $\varepsilon=52^\circ$ , from which we estimate an accuracy of  $\pm 0.01$  to  $\pm 0.02$ .

## 5. Discussion

We start from the hypothesis that there is the same type of dust everywhere in the inner solar system and that its radial distribution is given by a power law

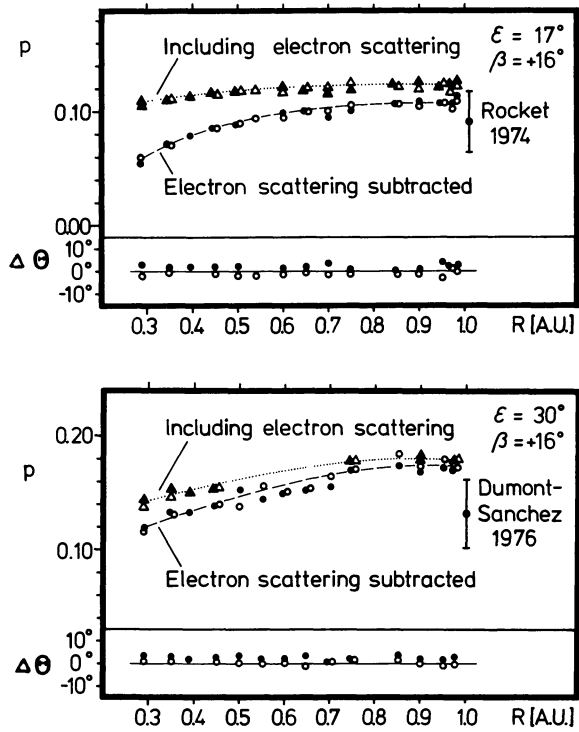
$$n(r, z) \sim r^{-\nu} \cdot f(|z/r|). \quad (9)$$

In this case

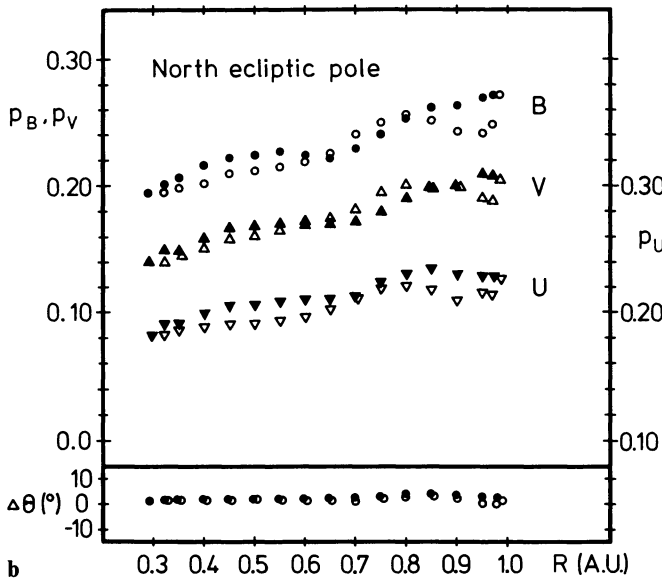
- the brightness increase towards the sun would be proportional to  $R^{-\nu-1}$  for all viewing directions,
- the colour would not change with  $R$
- the polarization also would remain constant.

The inverse is also true: strict fulfilment of conditions a)–c) proves the hypothesis (9) if we only accept that equal volume scattering functions also imply equal particle mixtures. Validity of condition a) alone still means that the scattering cross section per unit volume varies as  $r^{-\nu}$ .





a



b

**Fig. 9.** a Two examples for the change in polarization with heliocentric distance. Open symbols refer to observations east, filled symbols to observations west of the sun. The direction of polarization is given with respect to the normal to the scattering plane, counterclockwise on the sky. These are individual measurements in *B* selected for regular spacing in *R* from the inbound part of the first orbit of Helios 2. In the lower diagram some data points have been omitted for clarity. The rocket experiment is by Leinert et al. (1974, 1976). b Polarization of the zodiacal light at the north ecliptic pole as function of heliocentric distance during one orbit selected for good data coverage (October 11, 1976 to April 15, 1977). Filled symbols refer to the ingoing, open symbols to the outgoing part of the orbit.  $\Delta\theta$  as in Fig. a

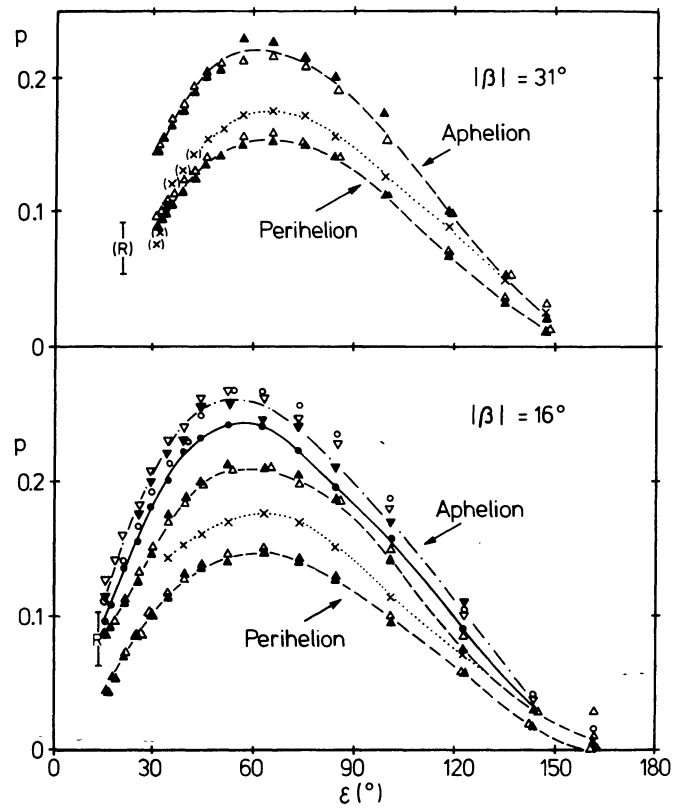


**Fig. 10.** Comparison of zodiacal light polarization observed around aphelion with the values in perihelion and with results from Dumont and Sanchez ( $\times$ ,  $\bullet$ ,  $\blacktriangle$  refer to *U*, *B*, and *V* measurements of Helios 2 (positive latitudes), open symbols to Helios 1. The rocket measurement at  $\epsilon=21^\circ$  is for an ecliptic latitude of  $\beta=21^\circ$ . At  $|\beta|=16^\circ$  the perihelion measurements in *U* and *B* have been omitted for clarity of the diagram. Each point represents an average over a period of two to three weeks around aphelion as read from a plot of results, containing observations east and west of the sun

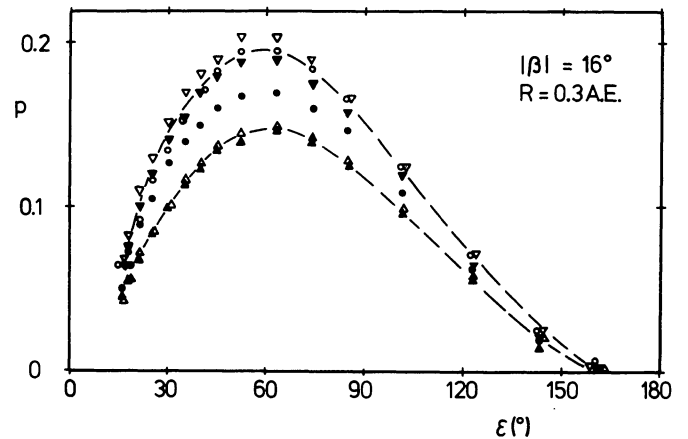


**Fig. 11.** Zodiacal light polarization at  $|\beta|=16^\circ$  observed in perihelion. Symbols are the same as in Fig. 10

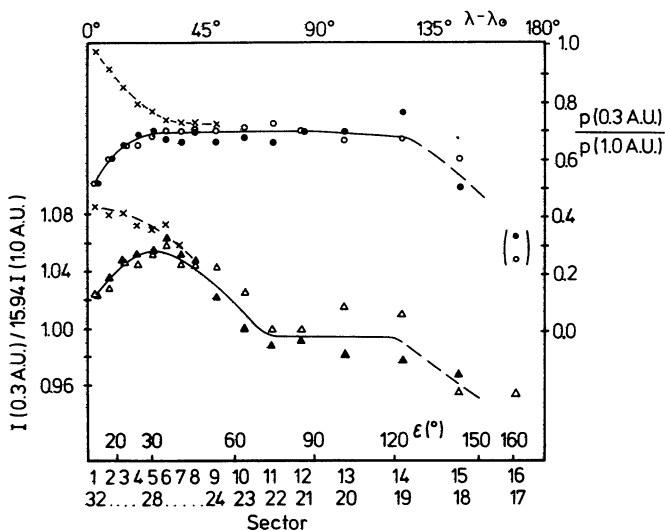


**Fig. 12.** Change of degree of polarization (○, ●) and intensity (△, ▲) of zodiacal light in  $V$  between 1.0 and 0.3 A.U. for ecliptic latitudes of  $\beta = \pm 16^\circ$ . Open symbols refer to Helios 1, filled symbols to Helios 2. The data points are calculated from Figs. 10, 2, and 3. The crosses result if electron scattering is corrected according to Eq. (10). A ratio of 15.94 of perihelion to aphelion intensities corresponds to  $I(R) \sim R^{-2.3}$

### 5.1. Spatial Distribution of Interplanetary Dust

From Fig. 5 we have  $I(R) \sim R^{-2.3 \pm 0.05}$  which means that  $\nu = 1.3$  within at least 1 A.U., with a slightly steeper increase inside 0.3 A.U. towards 0.09 A.U., the closest region accessible to Helios observations. The observed constancy of colours is compatible with a constant particle mixture of interplanetary dust, while the observed changes in polarization require some change in the particles. Nevertheless we suggest to accept the power law distribution (9) with  $\nu = 1.3$  as working model for the interplanetary dust. In the following we discuss in which direction the real distribution might deviate from this working model.

First one could try to link the observed decrease in polarization to a deficiency of particles with polar orbits near the sun. This would reduce the contribution of highly polarized  $90^\circ$ -scattering, thereby decreasing the observed polarization, particularly for the viewing directions closest to the sun. But this leaves us with the difficulty to explain the small extra brightness *increase* for exactly these viewing directions. Also the general decrease of polarization at larger elongations would still remain unexplained. We therefore feel that the changes in polarization are not primarily a product of spatial distribution.

Next we consider in more detail which impact the correction for interplanetary plasma may have on the derived spatial distribution. To this end we compare in Fig. 12, for ecliptic latitudes  $\beta = \pm 16^\circ$ , the change between aphelion and perihelion of degree of polarization and intensity of zodiacal light. We neglect the region  $\epsilon > 135^\circ$  because it is strongly affected by the difficulty to determine polarizations in aphelion. This leaves the two ranges  $\epsilon = 60\text{--}130^\circ$ , where the brightness increase is very close to the law  $I(R) \sim R^{-2.3}$ , and  $\epsilon < 60^\circ$ , where the increase is larger by about 5%. The dip in the intensity ratio towards sector 1 is not evident in Fig. 5 with its empirical normalization; it results from the normalization with help of Eq. (8). Electron scattering only is important for  $\epsilon < 45^\circ$ .

There we also considered the extreme case, that the dependence of electron density on heliographic latitude  $\phi$  would be

$$n(r, \phi)/n(r, 0) = 1.0 - \sin^{1/2} \phi \quad (10)$$

(Saito, 1970), which is zero (!) over the poles.

Therefore, in our opinion Eq. (2), which we used in our data analysis, is closer to reality, although it possibly exaggerates the plasma density over the poles. Figure 12 shows that with an intermediate correction for electron scattered light the additional decrease in polarization for the viewing directions closest to the sun could disappear, or even be changed into a relative increase. The influence on the brightness would be to emphasize a little more the steeper increase within 0.3 A.U. and correspondingly the increase in spatial density would have to be a little steeper. Uncertainties in the correction for interplanetary plasma are not important for the determination of the spatial distribution of dust.

One would expect that the zodiacal light observations performed between 1 A.U. and 3 A.U. by Pioneer 10 should smoothly connect to the Helios results. Indeed, the first evaluations for an elongation of  $\epsilon \approx 140^\circ$  (Hanner et al., 1976) are well represented by a spatial distribution of interplanetary dust  $n(r) \sim r^{-1.3}$  with a cut off at about 3 A.U. Schuerman (1980), however, in the range of elongations  $\epsilon = 70\text{--}170^\circ$  mostly found a steeper brightness decrease with heliocentric distance. But the example with  $I(R) \sim R^{-3.6 \pm 1.4}$ , which he presented, out to 2 A.U. closely follows the curve  $I(R) \sim R^{-2.3}$ , and it is only the observations around 3 A.U. at very low intensity levels ( $\leq 5$  S10) which steepen the line fit through the data points. In our opinion therefore the evidence is in favour of a continuation of the spatial distribution  $n(r) \sim r^{-1.3}$  out to at least 2 A.U.

The comparison with direct observations of interplanetary particles is affected by the flaw that these do not cover the size range of radii  $10\text{--}100 \mu\text{m}$  ( $10^{-8} \text{ g} - 10^{-5} \text{ g}$ ) which dominates the zodiacal light. Radio meteor observations (Southworth and Sekanina, 1973) refer to larger particles ( $10^{-5} - 10^{-2} \text{ g}$ ). In the range where the results are most reliable (0.7–2.0 A.U.) the authors find an increase of spatial density with heliocentric distance, opposite to our conclusions. On the other hand, the micrometeoroid flux ( $10^{-12} \text{ g} - 10^{-9} \text{ g}$ ) measured on board Helios 1 during 1975 is compatible with a spatial distribution  $\sim r^{-1.3}$  (Grün et al., 1977). Cook (1978), by tailoring a suitable dependence of particle albedo with heliocentric distance, forced the zodiacal light observations to fit the spatial distribution of radio meteors. This always is possible, mathematically, but it still leaves the discrepancy in spatial distribution with the micrometeorites. Cook did so because he took the radio meteors largely as responsible for the zodiacal light. Since Hanner (1980) shows that this mainly results from the low density of  $0.18 \text{ g/cm}^3$  Cook is using, there no longer exists a necessity to apply such methods of Procrustes. Instead, taking the results as they are, we find that the particles causing the zodiacal light are much more related to the micrometeoroids dynamically and in evolution than to the radio meteors.

### 5.2. Particle Properties

The reddening we found in the zodiacal light with respect to the solar spectrum appears to be typical of solid surfaces exposed to the environment of the solar system since a similar wavelength dependence was found for the albedo of Mercury (Vilas and McCord, 1976), lunar rocks and fines (Dollfus et al., 1971), Mars (McCord et al., 1977), asteroids (Bowell and Lumme, 1979), and meteorites (Gaffey and McCord, 1979). For the interplanetary par-

ticles in question, much larger than the wavelength of light and showing porous structure (Brownlee et al., 1980), such an effect therefore has to be expected caused by the wavelength dependence of the refractive index. At present we find it difficult to extract more information on grain material from our observed colours than this statement of general affinity.

However, a comment is possible on the model by Lamy and Perrin (1980) who conclude, on the basis of lunar microcrater counts by Morrison and Zinner (1977) and of measured depth to diameter ratios (Le Sergeant and Lamy, 1980), that about half of the zodiacal light is due to metallic submicron particles with a steep size distribution,  $n(a) \sim a^{-4.1}$ . The Mie calculations by Giese et al. (1973) for iron particles with  $n(a) \sim a^{-4.0}$ , in the range of radii 0.05–2.25  $\mu\text{m}$  should be representative for this particle population. They show that the contribution of such small particles to the zodiacal light should be bluer than the solar spectrum by about 20% both in  $B-V$  and  $V-R$  in the range of elongations 15–30°, approaching solar colour around  $\varepsilon=90^\circ$ . Both effects are opposite to what we observe. The argument from the observed zodiacal light colours is clearly against a dominating population of small particles in interplanetary space.

The polarization of zodiacal light observed by Helios (Fig. 10) is somewhat higher than previous out-of-ecliptic measurements. This tends to ease the modeling of zodiacal light which for compact spheres (Röser and Staude, 1978), absorbing porous (Giese et al., 1978) or nonabsorbing very tenuous particles (Greenberg and Gustafson, 1981) always leads to too high a polarization. The wavelength dependence of polarization is similar to that observed on lunar material, where Dollfus et al. (1971) found that the maximum polarization  $p_m$  is increasing with decreasing albedo  $A$  roughly as

$$p_m \sim A^{-1.55}. \quad (11)$$

In perihelion the reddening of the zodiacal light from  $U$  to  $V$  is 17% for a medium elongation of  $\varepsilon=90^\circ$ . Equation (11) then would predict the maximum polarization in  $U$  to be higher than in  $V$  by a factor of 1.3, which actually is the case. Although we have to make the reservation that we are measuring integrals over the line of sight, while Eq. (11) relates to single scattering, this emphasizes the general affinity between interplanetary dust and dust on the lunar surface seen above in the colours.

### 5.3. Changes with Heliocentric Distance

The general decrease of polarization towards perihelion obviously indicates a change in particle properties. Three effects might be at work which all relate to changes in the surface rather than in the particle material.

Increased roughness of the particles decreases the polarization as qualitatively discussed by Giese et al. (1978) and apparent in comparing measurements on lunar rocks and fines (Dollfus et al., 1971). But if the majority of interplanetary dust particles already is as porous 1 A.U. as shown by Brownlee et al. (1980), this effect should contribute very little. Greenberg and Gustafson (1981) found from laboratory measurements that mantles with low index of refraction around more refractive core particles greatly reduce the polarization of scattered light. Lunar micron-sized grains often have an about 500 Å thick amorphous radiation damaged coating produced by the solar wind (Maurette and Price, 1975). Such layers were shown by Hines and Arndt (1960) to have a lower refractive index than the original crystalline material. It then might be

speculated that such coating get the more important the closer the particles are to the sun and thus lead to reduced polarization. But for lunar material irradiation with protons resulted in a darker surface which, in turn, implied a higher polarization (Dollfus et al., 1971). The observed decrease of zodiacal light polarization with decreasing heliocentric distance to 70% of its value near 1 A.U. would then correspond, according to Eq. (11), to a 26% increase in reflectivity of the dust particles.

In summary we have to admit that we do not understand what change is taking part in interplanetary dust. As long as no at least partly convincing interpretation is available we tentatively ascribe the decreases in polarization to a change in the surface of interplanetary particles. The conclusion then still is a radial distribution  $n(r) \sim r^{-1.3}$  of interplanetary dust.

### 5.4. On the Importance of Collisions

The size distribution for an equilibrium under collisions is quite steep,  $n(a) \sim a^{-3.5}$  (Dohnanyi, 1972). Large collision rates therefore are expected to increase the importance of small particles for the zodiacal light particularly in the region closest to the sun where the number density is highest. We then should see a bluer colour, an increase in polarization and probably also an increase in intensity. In this context one is tempted to manipulate the correction for electron scattering in such a way that a 5–8% extra brightness increase for the zodiacal light close to the sun occurs, accompanied by some additional polarization (compare Fig. 12). But even so the observations set tight limits: a 7.5% extra increase in the intensity of sector 1 over the relation  $I(R) \sim R^{-2.3}$  only corresponds to a 10% increase of scattering cross section over the power law  $r^{-1.3}$  within 0.2 A.U. Also the colours (Fig. 6) clearly show no change. Our zodiacal light data do not indicate a dominant role of collisions for the destruction of interplanetary dust.

## 6. Conclusion

The discussion of the combined data of Helios 1 and Helios 2 has confirmed our earlier findings concerning the dependence of zodiacal light brightness on heliocentric distance. After correction for the effects of spacecraft orientation and of the symmetry plane of interplanetary dust the same power law  $I(R) \sim R^{-2.3}$  emerges with astonishing regularity for all viewing directions, the total brightness increase between 1.0 and 0.3 A.U. varying by only a few percent. These small variations correspond to differences in the exponent of the power law of mostly less than  $\pm 0.05$ . From this we infer a spatial distribution for the interplanetary dust of  $n(r, z) = r^{-1.3} f(|z/r|)$ , which should be valid not only for the range 0.3–1.0 A.U. covered by the Helios space probes but for the whole region 0.09–1.5 A.U. contributing significantly to the Helios observations. However, the pronounced decrease of zodiacal light polarization with decreasing heliocentric distance proves that the scattering particles cannot be exactly the same everywhere. We therefore consider the given spatial distribution as the best currently available working model, which may have to be modified once the effect on the polarization is at least partly understood. We want to emphasize that the proposed spatial distribution has a radial gradient steeper than  $1/r$ . This is a necessary condition for the interplanetary dust cloud to be in equilibrium, under the action of the Poynting-Robertson effect, with an extended source region. This might discriminate the interplanetary dust against the larger meteor particles. In this respect it may be meaningful that possible indicators of strong collisional activity, namely a bluer colour and a simultaneous

increase of brightness and polarization in the regions closest to the sun, are missing or at most marginally present in our data. Also the observed colours of the zodiacal light do not support a dominating abundance of submicron-sized particles. After all, collisions may not be as dominating for the evolution of interplanetary dust of sizes 10–100  $\mu\text{m}$  as usually is assumed. At least, the constraints given by our zodiacal light observations have to be considered when discussing the dynamics of interplanetary dust.

*Acknowledgements.* We thank Prof. Dr. H. Elsässer for continuous support and important suggestions during all of the project. M. Hanner developed most of the method of reduction. I. Mistrik, M. Al Makadsi, and R. Billing contributed a lot by programming, handling and reducing the data. The computations and data plots were performed at the computing facility of the Max-Planck-Institut für Kernphysik. This work was supported by the Bundesministerium für Forschung und Technologie with grant WRS 0108.

## References

- Allen, C.W.: 1946, *Monthly Notice Roy. Astron. Soc.* **106**, 137  
 Blanco, V.M., Demers, S., Douglass, G.G., Fitzgerald, M.P.: 1968, *Publ. U.S. Naval Obs.* **21**  
 Bowell, E., Lumme, K.: 1979, in *Asteroids*, ed. T. Gehrels, The University of Arizona Press, Tucson, p. 132  
 Brownlee, D.E.: 1980, in *Cosmic Dust*, ed. J. A. M. McDonnell, Wiley, Chichester, p. 275  
 Brownlee, D.E., Pilachowski, L., Olszewski, E., Hodge, P.W.: 1980, in *Solid Particles in the Solar System*, *Proc. IAU Symp.* **90**, eds. I. Halliday and B. A. McIntosh, Reidel, Dordrecht, p. 333  
 Burnett, G.: 1976, *Lecture Notes in Physics* **48**, 53  
 Classen, Ch.: 1976, Ph. D. Dissertation, Bonn  
 Coles, W.A., Rickett, B.I.: 1976, Goddard Space Flight Center Report X-660-76-53, p. 84  
 Cook, A.F.: 1978, *Icarus* **33**, 349  
 Dohnanyi, J.S.: 1972, *Icarus* **17**, 1  
 Dollfus, A., Geake, I.E., Titulaer, C.: 1971, in *Proc. Sec. Lunar Sci. Conf.*, ed. A. A. Levinson, *Geochim. Cosmochim. Acta, Suppl.* **2**, Vol. 3, p. 2285, MIT Press Cambridge, London  
 Dumont, R., Sanchez, F.: 1975, *Astron. Astrophys.* **38**, 405  
 Dumont, R., Sanchez, F.: 1976, *Astron. Astrophys.* **51**, 393  
 Dumont, R., L'Avasseur-Regourd, A.C.: 1978, *Astron. Astrophys.* **64**, 9  
 Edenhofer, P., Esposito, P.B., Hansen, R.T., Hansen, S.F., Lüneburg, E., Martin, W.L., Zyguelbaum, A.I.: 1977, *J. Geophys.* **42**, 673  
 Elsässer, H.: 1955, *Z. Astrophys.* **37**, 114  
 Elsässer, H.: 1958, *Mitt. Astron. Inst. Univ. Tübingen* Nr. 35  
 Fechtig, H., Hartung, J.B., Nagel, K., Neukum, G., Storzer, D.: 1974, in *Proc. Fifth Lunar Sc. Conf.*, *Geochim. Cosmochim. Acta Suppl.* **5**, Vol. 3, p. 2463  
 Frey, A., Hofmann, W., Lemke, D., Thum, C.: 1974, *Astron. Astrophys.* **36**, 447  
 Gaffey, M.J., McCord, Th.B.: 1979, in *Asteroids*, ed. T. Gehrels, University of Arizona Press, Tucson, p. 688  
 Gallouet, L.: 1964, *Ann. Astrophys.* **27**, 423  
 Giese, R.H.: 1973, *Planetary Space Sci.* **21**, 513  
 Giese, R.H., Hanner, M.S., Leinert, C.: 1973, *Planetary Space Sci.* **21**, 2061  
 Giese, R.H., Weiss, K., Zerull, R.H., Ono, T.: 1978, *Astron. Astrophys.* **65**, 265  
 Greenberg, J.M., Gustafson, B.A.S.: 1981, *Astron. Astrophys.* **93**, 35  
 Grün, E., Pailer, N., Fechtig, H., Kissel, J.: 1980, *Planetary Space Sci.* **28**, 333  
 Hoffleit, D.: 1964, *Catalogue of Bright Stars*, 3<sup>rd</sup> rev. ed. New Haven: Yale University Observatory  
 Grün, E., Fechtig, H., Kissel, J., Gammel, P.: 1977, *J. Geophys.* **42**, 717  
 Hanner, M.S.: 1980, *Icarus* **43**, 373  
 Hanner, M.S., Sparrow, J.G., Weinberg, J.L., Beeson, D.E.: 1976, *Lecture Notes in Physics* **48**, 29  
 Hines, R.L., Arndt, R.: 1960, *Phys. Rev.* **119**, 623  
 van de Hulst, H.C.: 1947, *Astrophys. J.* **105**, 471  
 Ingham, M.F.: 1961, *Monthly Notices Roy. Astron. Soc.* **122**, 157  
 Lamy, P.L., Perrin, J.M.: 1980, in *Solid particles in the solar system*, *Proc. IAU Symp.* **90**, eds. I. Halliday and B.A. McIntosh, Reidel, Dordrecht, p. 75  
 Leinert, C., Klüppelberg, D.: 1974, *Appl. Optics* **13**, 556  
 Leinert, C., Link, H., Pitz, E.: 1974, *Astron. Astrophys.* **30**, 411  
 Leinert, C., Link, H., Pitz, E., Salm, N., Klüppelberg, D.: 1975, *Raumfahrtforschung* **19**, 264  
 Leinert, C., Link, H., Pitz, E., Giese, R.H.: 1976, *Astron. Astrophys.* **47**, 221  
 Leinert, C., Hanner, M., Richter, I., Pitz, E.: 1980, *Astron. Astrophys.* **82**, 328  
 Leinert, C., Pitz, E., Link, H., Salm, N.: 1981, *J. Space Sci. Instr.* **5**, 257  
 Leinert, C., Richter, I.: 1981, *Astron. Astrophys.* (in press)  
 Le Sergeant, L.B., d'Hendecourt, Lamy, Ph.L.: 1980, *Icarus* **43**, 350  
 L'Avasseur, A.C., Blamont, J.: 1976, *Lecture Notes in Physics* **48**, 58  
 L'Avasseur-Regourd, A.C., Dumont, R.: 1980, *Astron. Astrophys.* **84**, 277  
 Lillie, Ch.F.: 1972, in *NASA SP-310*, ed. A. O. Code, Washington, p. 95  
 Link, H., Leinert, C., Pitz, E., Salm, N.: 1976, *Lecture Notes in Physics* **48**, 24  
 Mattila, K.: 1980, *Astron. Astrophys. Suppl. Ser.* **39**, 53  
 Maurette, M., Price, P.B.: 1975, *Science* **187**, 121  
 McCord, Th.B., Huguenin, R.L., Mink, D., Pieters, C.: 1977, *Icarus* **31**, 25  
 Morrison, D.A., Zinner, E.: 1977, *Proc. Lunar Sci. Conf. VIII*, p. 841  
 Pfeleiderer, J., Mayer, U.: 1971, *Astron. J.* **76**, 691  
 Pitz, E., Leinert, C., Link, H., Salm, N.: 1976, *Lecture Notes in Physics* **48**, 19  
 Pitz, E., Leinert, C., Schulz, A., Link, H.: 1979, *Astron. Astrophys.* **74**, 15  
 Roach, F.E., Megill, L.R.: 1961, *Astrophys. J.* **133**, 228  
 Röser, S., Staude, H.J.: 1978, *Astron. Astrophys.* **67**, 381  
 Saito, K.: 1970, *Ann. of the Tokyo Astron. Observatory Second Series*, Vol. XII, No. 2, 53  
 Schuerman, D.W.: 1980, in *Solid particles in the solar system*, *Proc. IAU Symp.* **90**, eds. I. Halliday and B. A. McIntosh, Reidel, Dordrecht, p. 71  
 Sharov, A.S., Lipaeva, N.A.: 1973, *Soviet Astron.* **17**, 69  
 Southworth, R.B., Sekanina, Z.: 1973, *NASA Contract Report CR-2316*  
 Sparrow, J.G., Ney, E.P.: 1968, *Astrophys. J.* **154**, 783  
 Sparrow, J.G., Ney, E.P.: 1972, *Astrophys. J.* **174**, 705  
 Sparrow, J.G., Weinberg, J.L.: 1976, *Lecture Notes in Physics* **48**, 41  
 Sparrow, J.G., Weinberg, J.L., Hahn, R.C.: 1976, *Lecture Notes in Physics* **48**, 45  
 Vilas, F., McCord, Th.B.: 1976, *Icarus* **28**, 593  
 Weinberg, J.L., Hahn, R.C.: 1980, in *Solid particles in the solar system*, *Proc. IAU Symp.* **90**, eds. I. Halliday and B. A. McIntosh, Reidel, Dordrecht, p. 19